Pricing European Call Options Using a Pseudospectral Method

Gunilla Linde, Martin Åberg

Report in Scientific Computing Advanced Course, spring 2004

Uppsala University
Department of Information Technology
Division of Scientific Computing

7th June 2004

Abstract

G. Linde, M. Åberg. 2004: Pricing European Call Options Using a Pseudospectral Method. Written in English. Uppsala, Sweden.

The aim of the project is to price European call options with a pseudospectral method (PS). An option is a financial asset that can be resembled to a lottery coupon. In a predefined time in the future the option is either worthless or worth more than it was bought for. Black–Scholes partial differential equation presented in 1973 was the main cause to the prestigious award Scholes was awarded in 1997, namely the Bank of Sweden Prize in Economic Science in Memory of Alfred Nobel. Since options diligently has been priced with the use of finite differences it works as a comparison to the results of PS. The set of points used when discretizing Black–Scholes equation is the Chebyshev points. The spatial convergence rate for PS is the same as for FD. When the initial condition is approximated with orthogonal Chebyshev polynomials and the domain is truncated the convergence rate increases significantly. The success is due to the transport of the maximum error to the region close to the left boundary and hence away from the exercise price, which is the region of most interest. Under these circumstances the maximum spatial error when using 100 grid points is of order 10^{-5} with PS compared to 10^{-2} with FD. The successful result in this work is achieved for the case when the option depends on one underlying asset. It would be of interest to try a more comprehensive approach than done in this work to expand it to more than one dimension.

Contents

1 Introduction

The aim of the project is to price European call options. A European call option is a contract with the following conditions:

- The holder of the option has at a prescribed time in the future, the expiry date (exercise date), the right to buy a prescribed asset. The asset is usually a stock which is bought for a prescribed amount, the exercise price (strike price).
- The holder of the option is in no way obliged to buy the underlying asset.
- The exercise price and the expiry date are determined at the time when the option is written.

Another type of option is American options. For an American call option the right to buy the underlying asset can be exercised at any time before the expiry date, not only at the expiry date which is the case for European options. The European/American classification has nothing to do with the continent of origin, it refers only to the technicality of when the option can be exercised. A put option gives the holder the right to sell a share of the underlying asset, in the same way as a call option gives the holder the right to buy the underlying asset. The owner of a call option wants the asset price to rise, because the higher the asset price is at expiry date the greater the profit will be. Analogously the owner of a put option wants the asset price to fall as low as possible.

An option gives the owner a right but no obligation, hence the option has a value and has to be paid for. Option pricing is all about answering the question *How much should one pay for this right?* How much an option is worth on the market depends on the time left to the expiry date and the price of the underlying asset.

An investor who believes that a particular stock will rise usually buy shares in that company. If he is correct he will make a profit and if he is wrong he loses money. If the share price rise from 250 SEK (Swedish crowns) to 270 SEK the profit will be 20 SEK or 8%. If the share price decrease to 230 SEK the loss will be 20 SEK or 8%. Alternatively the investor can buy a call option if he believes that the particular stock price will rise. For example if the investor buys an option with exercise price 250 SEK for 10 SEK and the stock price rise to 270 SEK at the expiry date he will make a profit of 10 SEK (270-250-10) or 100%. If the share price goes below the exercise price, the option is worthless and the investor loses all the invested money, in this example 10 SEK or 100%. The region around the exercise price is of certain interest because it is close to the estimate of the underlying asset,

and it makes the difference between a profit and a loss. Options can be a cheap way of exposing a portfolio to a large amount of risk. With options it is also possible to make money, although the stock price falls. [1],[6]

The price of an option can be determined by solving Black–Scholes partial differential equation (PDE). The equation was presented in 1973 by Fischer Black and Myron Scholes. Since then the original Black and Scholes option pricing model has been the subject of much attention. Many financial scholars, among them Robert Merton, have expanded the original work and relaxed assumptions required in the original model. In 1997 Merton and Scholes were awarded the Bank of Sweden Prize in Economic Sciences in Memory of Alfred Nobel. Black, who died in 1995, would undoubtedly have shared the prize with Merton and Scholes if he had been alive. [3],[4]

The parabolic PDE is solved in one and two dimensions using finite differences and pseudospectral Chebyshev. In one dimension the analytic solution is used for comparisons with the numerical solutions from both methods.

This report is organized as follows. The Black–Scholes equation and numerical methods are described in section 2. The results for the one dimensional case are presented in section 3, and the two dimensional case in section 4. The report is completed with a discussion in section 5.

2 Theory

2.1 The Black–Scholes equation

To be able to derive Black–Scholes equation it is necessary to have a model of the option market. The Black–Scholes model for the financial market is:

$$dB(t) = rB(t)dt \tag{1}$$

$$dS(t) = \alpha S(t)dt + \sigma S(t)dW(t) \tag{2}$$

B is the price process of a risk free asset, S is the price process of a stock and t is the time. The constants r, α and σ are deterministic given. Where r is interpreted as the interest rate and σ is known as the volatility and describes the tendency of the asset to change value. The local mean rate of return of S is denoted α. W is a Wiener process which is a stochastic process containing the randomness that is a feature of the asset price. [6]. A Wiener process, $W(t)$, fulfills:

- it is a continuous time stochastic process for $t \geq 0$,
- $W(0) = 0$,
- $W(t) - W(s) \in \mathcal{N}(0, \sqrt{t-s})$ for any $0 \leq s < t$,

- increments for nonoverlapping time intervals are independent.

A random walk with random step sizes is the most common example of a Wiener process. [9]. As opposed to the risk free asset, the stock has a stochastic rate of return simulated by the Wiener process. [6]

The assumptions used in Black–Scholes model are:

- the stock pays no dividends during the option's life,
- markets are efficient,
- no commissions are charged, hence no transaction costs exist,
- interest rates remain constant and known,
- returns on the underlying stock are normally distributed. [4]

An efficient market is a market free of arbitrage possibilities. An arbitrage possibility is the possibility of making a positive amount of money out of nothing with probability 1. Black–Scholes model of the financial market is used together with Itô calculus to derive Black–Scholes equation [1], [6]

$$F_t(s,t) + rsF_s(s,t) + \frac{s^2\sigma^2}{2}F_{ss}(s,t) - rF(s,t) = 0 \tag{3}$$

$$F(s,T) = \max(s-K,0) \tag{4}$$

in the domain

$$[0, S_{max}] \times [0,T]. \tag{5}$$

In equation (3),(4) F is the value of the option, K is the strike price and subscripts denote partial derivatives. The expiry date is denoted by T and s is the price of the underlying stock. There does not exist an initial condition for Black–Scholes equation, which is usually the case for PDEs describing physical phenomena. Instead it is the value of the option at present time ($t = 0$) which is to be determined. The value of the option at the exercise date T is known and stated in equation (4). The final condition given in equation (4) is graphically presented in Figure 1.

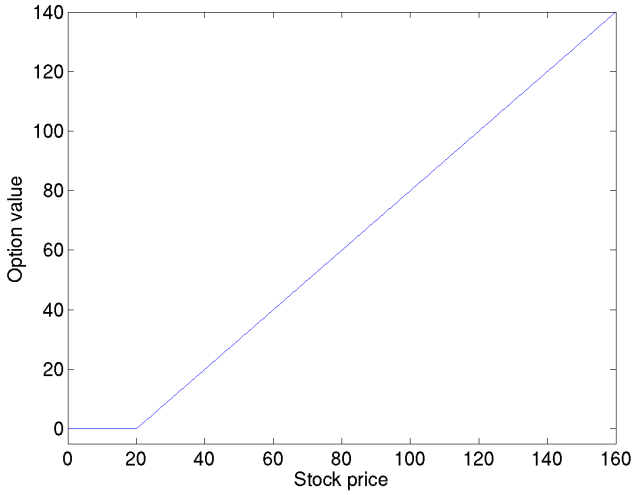

Figure 1: The final condition. The value of the option at the time of exercise as a function of the stock value. The strike price used is $K = 20$.

If the asset is worth more than the strike price on the day of exercise it makes sense to exercise the option. The holder of the option can buy the stock for the exercise price and immediately sell it at the stock market. The profit will be the difference between the stock price and the exercise price. For example, if the exercise price is 50 SEK and the stock price is 100 SEK at the time of exercise, the profit will be 50 SEK. The option is therefore valued to 50 SEK. If the asset is worth less than the strike price there is no meaning to exercise the option. Why exercise the option and pay 50 SEK for a stock when it can be bought for 40 SEK at the stock market? In this case the value of the option is 0 SEK.

Zero as the lower boundary for s, equation (5), comes from the fact that the value of the underlying asset cannot become negative. There is no natural upper limit for s. The value of the stock can rise without boundary, but it is not likely. Numerical methods work on a bounded domain, hence an artificial boundary at S_{max} is introduced. We usually choose $S_{max} = 8K$. The domain in time is straight forward, it goes from today,$t = 0$, to the exercise date, $t = T$.

2.1.1 Analytic solution

If the option only depends on one underlying asset Black–Scholes equation is one-dimensional. In the case when the equation is one-dimensional and the interest rate and the volatility are constant there exist an analytic solution.

If the option depends on more than one underlying asset Black–Scholes equation is multi-dimensional. Then no analytic solution exist and it is necessary to solve the problem with numerical methods.

To solve equation (3) in the one-dimensional case the following changes of variables are used:

$$s = Ke^x, \quad t = T - \frac{2\tau}{\sigma^2}, \quad F = Kv(x,\tau) \tag{6}$$

and the Black–Scholes equation is transformed into

$$\frac{\partial v}{\partial \tau} = \frac{\partial^2 v}{\partial^2 x} + (\frac{2r}{\sigma^2} - 1)\frac{\partial v}{\partial x} - \frac{2r}{\sigma^2}v. \tag{7}$$

The final condition, equation (4), is transformed into the initial condition:

$$v(x,0) = \max(e^x - 1, 0).$$

With the change of variables presented in equation (6), equation (7) is close to the diffusion equation. By putting:

$$v(x,\tau) = e^{\alpha x + \beta \tau} u(x,\tau) \tag{8}$$

equation (7) is turned into the diffusion equation which has a well known solution, see [1]. In the solution of the diffusion equation a final change of variables back to the original variables are made and the analytic solution is

$$F(s,t) = s\mathcal{N}(d_1) - Ke^{-r(T-t)}\mathcal{N}(d_2) \tag{9}$$

where

$$d_1(s,t) = \frac{1}{\sigma\sqrt{T-t}}\left(\ln\frac{s}{K} + (r + \frac{\sigma^2}{2})(T-t)\right),$$

$$d_2(s,t) = d_1(s,t) - \sigma\sqrt{T-t}$$

and $\mathcal{N}(x)$ is the cumulative normal distribution function:

$$\mathcal{N}(x) = \frac{1}{\sqrt{2\pi}}\int_{-\infty}^{x} e^{\frac{-y^2}{2}} dy.$$

Equation (9) is hence the explicit solution of the Black–Scholes PDE. For more details of the derivation of the analytic solution see [1].

2.1.2 Black–Scholes equation in higher dimensions

When the option depends on two different stocks Black–Scholes equation becomes 2-dimensional and hence if the option depends on d number of stocks the equation is d space-dimensional. Black–Scholes 2-dimensional equation is

$$\begin{aligned}&\frac{\partial F}{\partial t} + s_1 r \frac{\partial F}{\partial s_1} + s_2 r \frac{\partial F}{\partial s_2} + \frac{1}{2}\left[\sigma\sigma^*\right]_{11} s_1^2 \frac{\partial^2 F}{\partial s_1^2} + \frac{1}{2}\left[\sigma\sigma^*\right]_{22} s_2^2 \frac{\partial^2 F}{\partial s_2^2} + \\ &\left[\sigma\sigma^*\right]_{12} s_1 s_2 \frac{\partial^2 F}{\partial s_1 \partial s_2} - rF = 0\end{aligned} \tag{10}$$

and the d space-dimensional equation is [7]

$$\frac{\partial F}{\partial t} + \sum_{i=1}^{d} r s_i \frac{\partial F}{\partial s_i} + \frac{1}{2}\sum_{i,j=1}^{d}\left[\sigma\sigma^*\right]_{ij} s_i s_j \frac{\partial^2 F}{\partial s_i \partial s_j} - rF = 0. \tag{11}$$

σ^* is the transpose of the symmetric matrix σ. In two dimensions σ is

$$\sigma = \begin{bmatrix} \sigma_{11} & \sigma_{12} \\ \sigma_{21} & \sigma_{22} \end{bmatrix}$$

where σ_{11} is the volatility for stock 1 and σ_{22} is the volatility for stock 2. σ_{12} is the correlation between the two underlying stocks. The final condition for the basketoption with equal weights on the underlying assets

$$F(s_1, s_2, T) = \max\left(\frac{s_1 + s_2}{2} - K, 0\right). \tag{12}$$

In higher dimensions no general analytic solution exists.

2.1.3 Temporal transformation

The original Black–Scholes equation, equation (3), is backward in time. Instead of taking negative time steps the problem is transformed to become forward in time. The change of variable

$$\tau = T - t,$$

transform equation (3), (4) to:

$$F_\tau(s, \tau) = rsF_s(s, \tau) + \frac{s^2\sigma^2}{2}F_{ss}(s, \tau) - rF(s, \tau) \tag{13}$$

$$F(s, 0) = \max(s - K, 0). \tag{14}$$

2.2 Spatial and temporal discretization using finite differences

Equation (13) is discretized by finite differences (FD) in space and time. The first order and the second order derivative in space is approximated with central differences, both of second order accuracy. Time is discretized by the backward Euler, which is unconditionally stable and of accuracy order one. The left-hand side of equation (13) is thus approximated with:

$$F_\tau(\tau, s) = \frac{F^{n+1} - F^n}{\Delta\tau} + \mathcal{O}\left((\Delta\tau)^2\right). \tag{15}$$

The superscript n refers to the time level. Using equation (15) to discretize equation (13) results in:

$$\frac{F^{n+1} - F^n}{\Delta\tau} = rsD_0F^{n+1} + \frac{s^2\sigma^2}{2}D_+D_-F^{n+1} - rF^{n+1} \Rightarrow \tag{16}$$

$$(I - \Delta\tau rsD_0 - \Delta\tau\frac{s^2\sigma^2}{2}D_+D_- + \Delta\tau rI)F^{n+1} = F^n, \tag{17}$$

where the central differences used are:

$$D_+D_-F_j^n = \frac{F_{j+1}^n - 2F_j^n + F_{j-1}^n}{(\Delta s)^2}, \tag{18}$$

$$D_0F_j^n = \frac{F_{j+1}^n - F_{j-1}^n}{2\Delta s}, \qquad j = 0, \ldots, N. \tag{19}$$

The space domain is discretized with $N + 1$ equidistant points when using finite differences. The subscript j describes a point s_j in the space domain. The expression between brackets in equation (17) is a matrix which is denoted by A. It is now straightforward to get the solution for the next time step by solving the system of equations

$$AF^{n+1} = F^n. \tag{20}$$

Second order backward differenced formula, BDF2, can be used instead of Euler backward when discretizing in time. BDF2 is an implicit unconditionally stable method with accuracy order 2 instead of order 1 for Euler backward. The left-hand side of equation (13) approximated with BDF2

$$F_\tau(\tau, s) = \frac{F^{n+2} - \frac{4}{3}F^{n+1} + \frac{1}{3}F^n}{\frac{2}{3}\Delta\tau} + \mathcal{O}\left((\Delta\tau)^3\right). \tag{21}$$

The A-matrix for BDF2 looks like:

$$A = \Big(I - \frac{2}{3}(\Delta\tau r s D_0 + \Delta\tau \frac{s^2\sigma^2}{2} D_+ D_- - \Delta\tau r I)\Big).$$

The system of equations arising from the discretization with BDF2 of equation (13) is:

$$AF^{n+2} = \Big(\frac{4}{3}F^{n+1} - \frac{1}{3}F^n\Big). \tag{22}$$

The drawback using BDF2 is that the method uses two time levels to calculate the solution for the new time level. Therefore another method is needed to start up BDF2, here Euler backward is used.

2.3 Spatial discretization using a pseudospectral method

Pseudospectral methods (PS) for solving partial differential equations uses global basis functions, whereas finite differences are local approximations. PS methods initially uses N collocation points. The function values of the N points are used to determine an interpolated polynomial of degree $\leq N$. The spatial derivatives in the PDE are approximated by the derivatives of the polynomials.

The typical convergence rate of spectral methods for smooth functions is $\mathcal{O}(N^{-m})$ for all real m. For analytic functions the convergence rate is $\mathcal{O}(c^N)$ $(0 < c < 1)$. Such behavior is known as spectral accuracy or spectral convergence [2]. In Black–Scholes equation the initial condition is not a smooth function, the first derivative is discontinuous at K. With F' discontinuous, the error near the irregularity will be of order 1 and of order 2 in the rest of the domain [5].

The simplest approach would be to use N equidistant points. When N increase, the errors increase exponentially, called the Runge phenomenon, for details see [2]. To achieve spectral accuracy when using pseudospectral methods one should instead use polynomial interpolation in unevenly spaced points. The points are distributed with the density:

$$density \sim \frac{N}{\pi\sqrt{1-x^2}}.$$

The Chebyshev points fulfill this requirement. But the main advantage of using the Chebyshev points is the freedom to use different types of boundary conditions. Especially appropriate to use with Chebyshev are Dirichlet Boundary conditions. The Chebyshev points are defined by:

$$x_j = \cos(j\pi/N), \qquad j = 0, \ldots, N. \tag{23}$$

The Chebyshev polynomials are given by:

$$T_n(x) = \cos(n \arccos(x)), \qquad -1 < x < 1, \qquad n = 0, 1, 2, \ldots \tag{24}$$

and the first three ones are:

$$\begin{cases} T_0 = 1 \\ T_1 = x \\ T_2 = 2x^2 - 1. \end{cases}$$

The Chebyshev polynomials are orthogonal according to [8]:

$$\int_{-1}^{1} \frac{T_i(x)T_j(x)}{\sqrt{1-x^2}} dx = \begin{cases} 0, & i \neq j \\ \pi, & i = j = 0 \\ \pi/2, & i = j \neq 0. \end{cases} \tag{25}$$

Orthogonality for discrete function values:

$$\sum_{k=1}^{M} T_i(x_k)T_j(x_k) = \begin{cases} \frac{1}{2}M\delta_{ij}, & i,j \neq 0, \qquad i,j \leq M \\ M, & i = j = 0. \end{cases} \tag{26}$$

The Chebyshev polynomials, T_n, are defined in the domain $[-1, 1]$. The domain used in the original problem, equation (5), is transformed by the substitution

$$x = \frac{2s}{S_{max}} - 1. \tag{27}$$

According to Weierstrass approximation theorem [10] an arbitrary function that is continuous can be described by a linear combination of Chebyshev polynomials:

$$F(x,t) = \sum_{j=0}^{\infty} c_j(t)T_j(x), \tag{28}$$

where c_j is defined as:

$$c_j =< F, T >= \int_{-1}^{1} \frac{F(x,t)T_j(x)}{\sqrt{1-x^2}} dx. \tag{29}$$

To be able to use equation (28) with a finite number of Chebyshev polynomials we introduce P_N, which includes the error term caused by the limited number of polynomials used. The changed coefficient vector is denoted by $\tilde{c}_j$ and defined as follows:

$$P_N F(x,t) = \sum_{i=0}^{N} \tilde{c}_i(t) T_i(x), \tag{30}$$

$$\tilde{c}_0(t) \equiv \frac{1}{M} \sum_{k=1}^{M} F(x_k, t), \tag{31}$$

$$\tilde{c}_i(t) \equiv \frac{2}{M} \sum_{k=1}^{M} F(x_k, t) T_i(x_k), \qquad i = 1, \ldots, N \tag{32}$$

$$x_k = \cos\Big(\frac{\pi(k-1/2)}{n}\Big), \qquad k = 1, \ldots, n \tag{33}$$

$$M \geq N.$$

By using equation (28) together with equation (31) the following expression for the coefficients $\tilde{c}_i$ is derived.

$$\begin{aligned} \tilde{c}_i(t) = & \sum_{k=1}^{M} \sum_{j=0}^{\infty} c_j(t) T_j(x_k) T_i(x_k) = \\ & \sum_{k=1}^{M} \sum_{j=0}^{N} c_j(t) T_j(x_k) T_i(x_k) + \sum_{k=1}^{M} \sum_{j=N+1}^{\infty} c_j(t) T_j(x_k) T_i(x_k) = \\ & c_i(t) + \sum_{k=1}^{M} \sum_{j=N+1}^{\infty} c_j(t) T_j(x_k) T_i(x_k), \qquad i = 1, \ldots, N. \end{aligned} \tag{34}$$

The coefficients $\tilde{c}_i$ from equation (34) is inserted into equation (30) and orthogonality of Chebyshev polynomials is used.

$$P_N F(x,t) = \sum_{i=0}^{N} c_i(t) T_i(x) + \sum_{i=0}^{N} \sum_{k=1}^{M} \sum_{l=N+1}^{\infty} c_l(t) T_l(x_k) T_i(x_k) T_i(x).$$

If equation (30) is multiplied with a series of orthogonal Chebyshev polynomials $\tilde{c}_i$ becomes:

$$\begin{cases} \tilde{c}_0(t) \simeq \frac{1}{M} \sum_{k=1}^{N} F(x_k, t) \\ \tilde{c}_i(t) \simeq \frac{2}{M} \sum_{k=1}^{N} F(x_k, t) T_j(x_k), \qquad j = 1, \ldots, N. \end{cases} \tag{35}$$

The initial state is given, therefore the coefficients $c_i(0)$ are known. Hence the initial error of this method is:

$$\varepsilon = \| F(x_k,0) - P_N F(x_k,0) \| = \| F(x_k,0) - \sum_{j=0}^{N} c_j(0) T_j(x_k) \|$$
$$+ \| \sum_{i=0}^{N} \sum_{k=1}^{M} \sum_{l=N+1}^{\infty} c_l(0) T_l(x_k) T_i(x_k) T_i(x) \|, \qquad i,k = 1,\ldots,N.$$

When studying the coefficients c_j in Figure 2 it is clear that they decrease when j increase. For $M \geq 10N$ the last term of the error ε becomes infinitesimal and the approximation below can be made

$$\varepsilon \simeq \| F(x_k,0) - \sum_{j=0}^{N} c_j(0) T_j(x_k) \| . \tag{36}$$

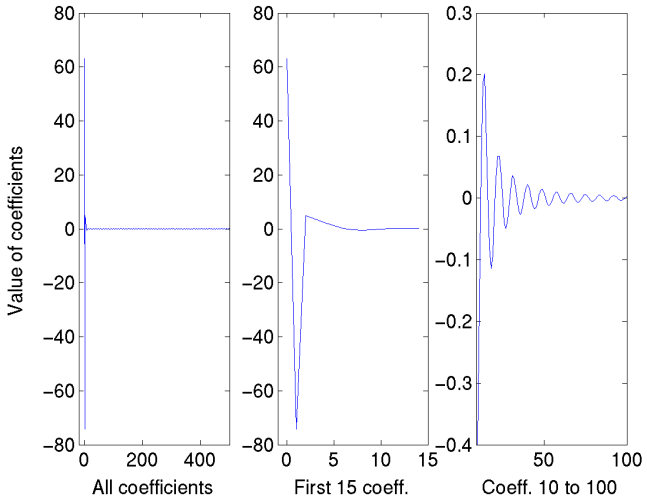

Figure 2: Value of coefficients c_j for a polynomial approximation of the initial condition. Notice the scale on the third graph.

As mentioned above the spatial derivatives for the pseudospectral method with the Chebyshev polynomials are given by the derivatives of the Chebyshev polynomials. The differentiation matrix, for the discretization of the first order derivative in space, is defined as follows [2].

$$
\begin{aligned}
(D_N)_{00} &= \frac{2N^2+1}{6}, \qquad (D_N)_{NN} = -\frac{2N^2+1}{6}, \\
(D_N)_{jj} &= -\frac{-x_j}{2(1-x_j^2)}, \qquad j = 0, \ldots, N, \\
(D_N)_{ij} &= \frac{c_i}{c_j}\frac{(-1)^{i+j}}{(x_i - x_j)}, \qquad i \neq j \qquad i, j = 0, \ldots, N.
\end{aligned}
$$

The differentiation matrix for the second order derivative in space is D^2.

3 Results in one dimension

The default parameters used are: $\sigma = 0.3$, $\Delta\tau = 0.01$, $K = 20$, $S_{max} = 8K$, $r = 0.05$ and $T = 1$ year. When nothing else is stated BDF2 is used to iterate in time.

3.1 Boundary conditions

When solving Black–Scholes PDE with FD one possible boundary condition is to use $\frac{\partial^2 F}{\partial s^2} = 0$, both at the left and the right boundary point. The same boundary condition was tried when solving with PS, but resulted in an unpredictable behavior at the right boundary. The reason is that when using the boundary condition $\frac{\partial^2 F}{\partial s^2} = 0$ with PS the solution at the first time level must also fulfill this criteria, which is not the case initially in this problem. We believe it is possible to fulfill this criteria, but it seems very technically and hence beyond the scope of this work. Instead

$$
F(0,t) = 0, \qquad F(S_{max}, t) = S_{max} - Ke^{-rt} \tag{37}
$$

was used as boundary condition when solving the PDE with PS. As mentioned in section 2.3 Dirichlet boundary conditions are especially appropriate to use together with Chebyshev points. If this is the case in this problem, is studied by solving the Black–Scholes PDE, first with the use of Dirichlet boundary condition and secondly with the analytic boundary condition from equation (9). Figure 3 below shows that the Dirichlet boundary condition results in almost exactly the same solution as the solution with analytic boundary condition. The maximum difference between the two solutions is of the order 10^{-12} for all N. Because there exist an analytic solution only in the one dimensional case it is not possible to generalize the analytic boundary condition into more dimensions. Therefore it is of great importance that the Dirichlet boundary condition can be used.

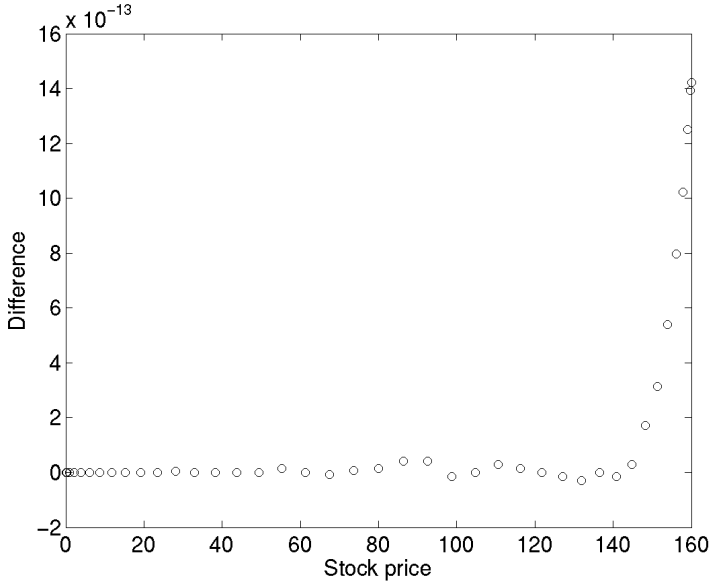

Figure 3: The difference in the solution of the PDE when Dirichlet and analytic boundary conditions are used. The number of grid points used were 40.

3.2 Finite differences

When using finite differences with equidistant points in space to solve the Black–Scholes discretized PDE, the maximum error is centered around the exercise price (Figure 4 top). This is a big drawback because the region around the exercise price is of special interest. Therefore it would be an advantage to either spread out the error or move the error to another region.

The discretization method used is of second order accuracy (section 2.2). If the step length is halved the error is reduced by a factor 4. The bottom half of Figure 4 shows that the spatial convergence is as expected. The reason that the error is centered around K is because the initial condition is discontinuous in the first derivative at the exercise price.

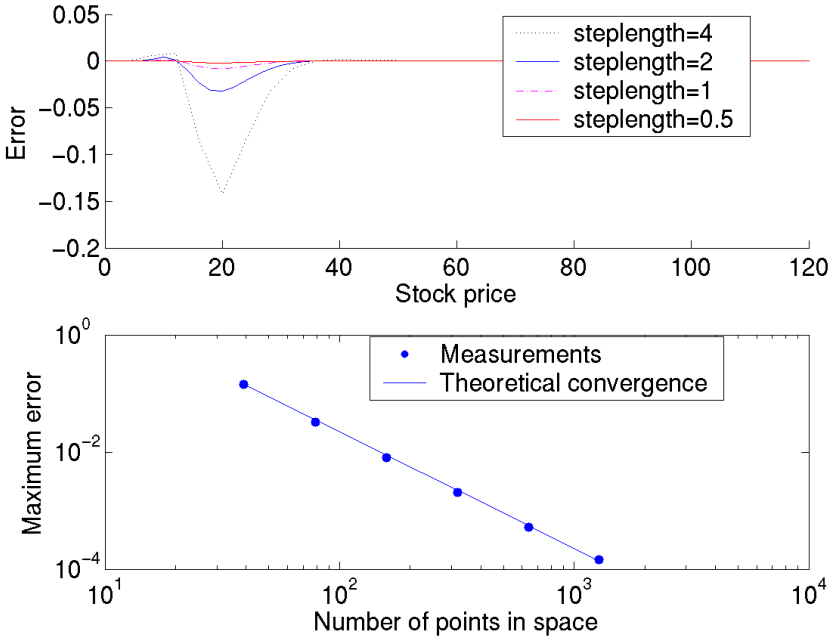

Figure 4: The top figure describes the error as a function of stock price for different distances between grid points in space. The bottom figure describes the rate of spatial convergence for the maximum error.

When the number of grid points is kept constant and $\Delta\tau$, the step length in time, is reduced the measured rate of convergence is 2 for BDF2 and 1 for Euler backward, in agreement with theory (section 2.2). When measuring the rate of spatial convergence it is important that the time discretization error is of lower magnitude than the spatial error. This is done by choosing $\Delta\tau$ sufficiently small. If the errors are of the same magnitude, the error from the time discretization hide the reduction of the spatial error, and the convergence of the spatial error cannot be discerned. The error measured is the combination of the error from time and spatial discretizing. Analogously when studying the rate of convergence for the time discretization, Δs has to be chosen sufficiently small, to not hide the reduction of the time discretization error.

3.3 Pseudospectral - representation error of the initial condition

When discretizing in space with the pseudospectral method the error of the solution is centered around K, the same behavior as for the case with finite

differences. As mentioned in section 2.3, PS uses polynomials to approximate functions. The initial condition equation (4) is thus approximated with polynomials. Hence the representation error at $t = 0$, is the difference between the IC and the approximation. Figure 5 below shows this error or difference when the IC is approximated with polynomials of degree $N - 1$, where N is the number of grid points used.

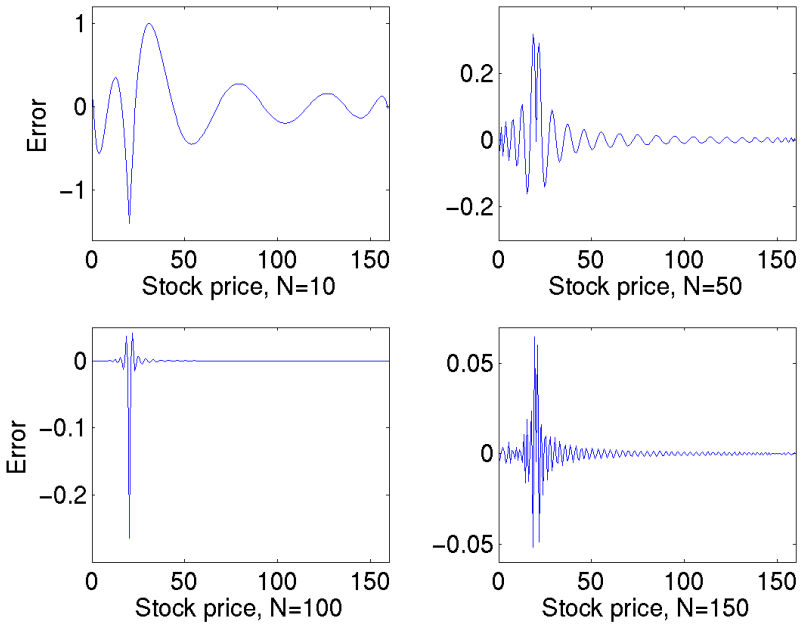

Figure 5: Representation error for different number of grid points.

Even in the case when many grid points are used to approximate the IC the error is still significant. This is the result of trying to fit polynomials to a function that is not smooth. When solving equations numerically a more accurate start often results in a more accurate solution. In the one-dimensional case the PDE has an analytic solution, see section 2.1.1. Therefore it is straightforward to investigate if there exist a correlation between the representation error and the error when the PDE is solved. When studying Figure 6 below it is obvious that there exist a correlation that leads to the conclusion that the representation error should be minimized to achieve a more accurate solution.

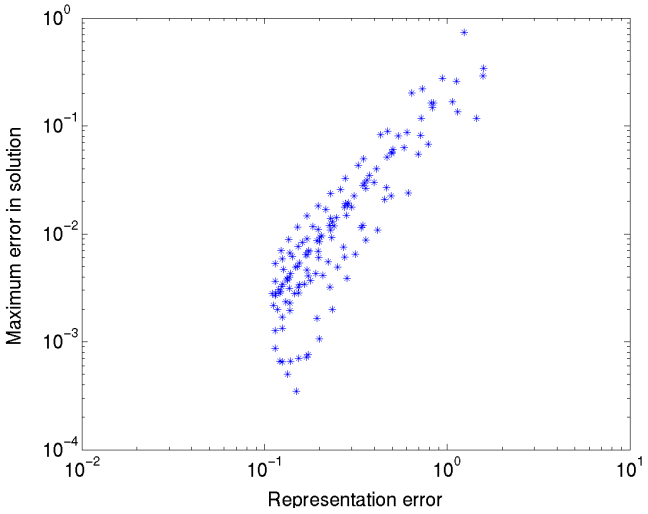

Figure 6: Correlation between the maximum representation error and the maximum error in the solution.

3.3.1 Minimizing the representation error

The most straightforward way to reduce the representation error is to increase the number of grid points used. The downside of this method is that the convergence of the representation error is only of order 1, as shown in Figure 7 below, this is in agreement with theory [5].

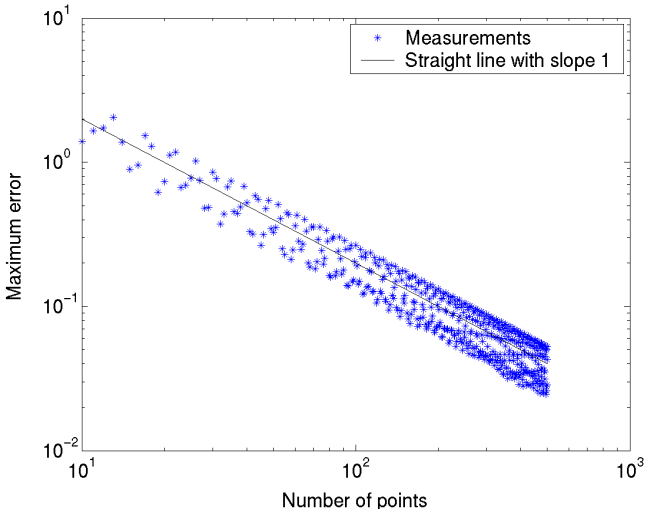

Figure 7: Convergence of the representation error.

As mentioned earlier the maximum error is situated at K. Figure 7 shows that the error decrease when the number of grid points increase, but when studying the figure carefully one can see an oscillative behavior of the error. Because the maximum error appears at K, it is of interest to study the location of the neighboring points relative to K both from the right-hand side and the left-hand side. The locations and the distances to K are defined in Figure 8 below.

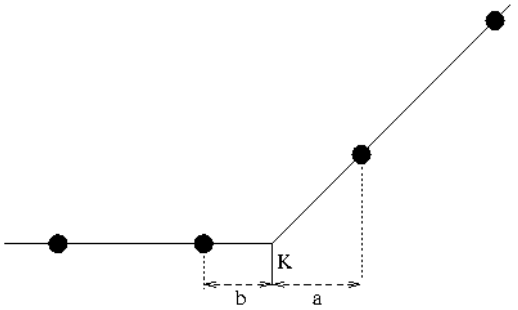

Figure 8: Definition of distance a and b.

The oscillative behavior is correlated with the distances a and b. Figure 9 below, shows that a grid point close to the exercise price results in a lower representation error than if the grid points are farther away. It does not matter if it is the right or the left grid point that is close to K. The distances plotted in Figure 9 are scaled with a factor $\frac{1}{6}$ to be of the same magnitude as the error. The Chebyshev points are defined according to equation (23), and therefore it is not possible to place the points at the preferred distances with this method. A possible approach would be to use another set of points when using pseudospectral methods but that is beyond the scope of this work.

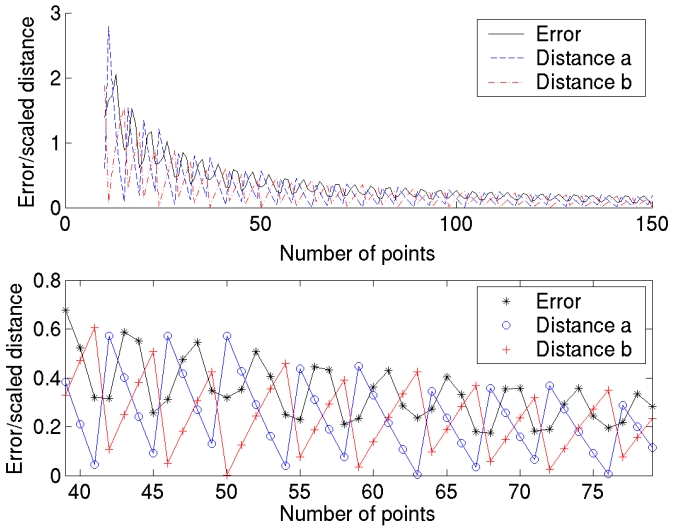

Figure 9: Correlation between representation error and the smallest distance between a grid point and the exercise price. The distances are scaled with a factor $\frac{1}{6}$.

The default value for S_{max} when solving the PDE in this work is set to eight times the value of K. Figure 10 below, shows how the maximum error changes when the domain is increased from $[0, 80]$ to $[0, 240]$. The choice of domain do not have a large impact on the accuracy when a sufficient number of grid points are used.

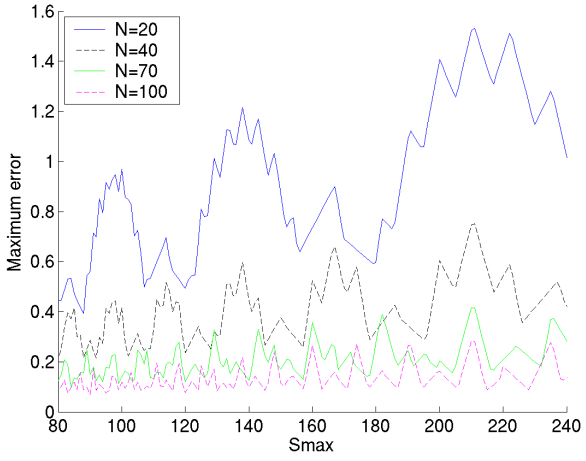

Figure 10: Representation error for different S_{max}.

The IC is approximated with equation (30). The number of coefficients for the approximation is M. To achieve a better approximation, M in equation (31) is chosen bigger than N, which is presented in Figure 11 below.

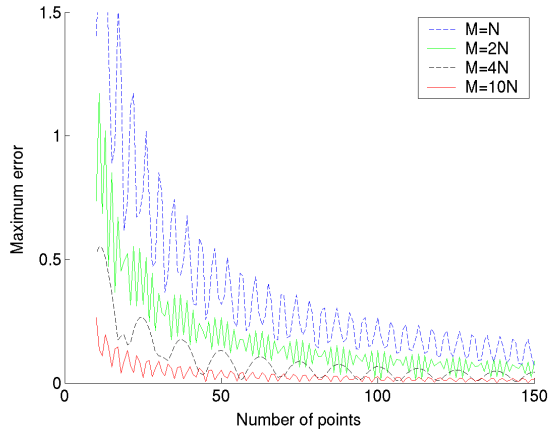

Figure 11: Representation error for M coefficients used.

When the PDE is solved the number of grid points used are N. Therefore when the IC is approximated in equation (30) the number of coefficients used should be the same as the number of grid points. This is not the case in Figure 11 where all coefficients are used for the approximation. In Figure 12 below the coefficients used in the approximation are restricted to the number of grid points. When M is chosen at least four times bigger than N the oscillative behavior of the maximum error disappears.

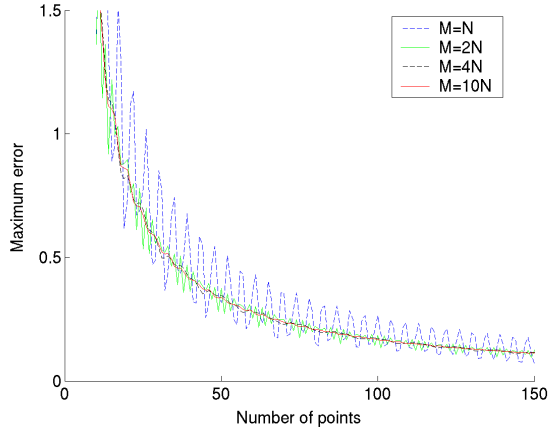

Figure 12: Representation error when the first N coefficients are used.

As seen in Figure 12 the oscillative behavior of the maximum error vanish when M increases. This is the result of better approximated coefficients c_j, defined in equation (31). When choosing M to achieve a maximum error of sufficient accuracy it is of interest to study how the coefficients converge when M increases, Figure 13 below.

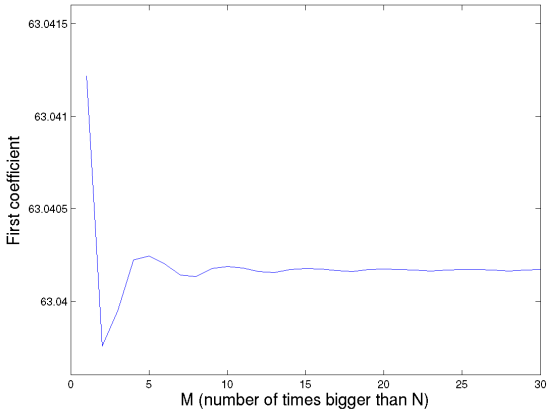

Figure 13: Convergence for coefficient c_0.

The cost to reduce the representation error by using M greater than N is small, since the calculations is only done once. Compared with increasing N which results in a larger system of equations to be solved in every iteration in time.

3.4 Comparison of solution with the use of finite differences and a pseudospectral method

As mentioned in section 3.3.1 the representation error decrease when the number of coefficients M evaluated are greater than the number of grid points N. From here on the notation PS simply refers to when the PDE is solved with the IC from the original equation. And PS approximated IC refers to when M is greater then N.

Since there exist an analytic solution to the PDE in the one-dimensional case, it is easy to compare the accuracy of the numerical solutions obtained from FD, PS and PS approximated IC. Preferably the difference between the analytic solution and the numerical solutions will decrease when iterating forward in time. Figure 14 shows that the maximum error for PS approximated IC decreases with the highest rate. The bottom picture is a magnification of the one in the middle but with logarithmic axis. It clearly shows how the maximum error for PS approximated IC decreases.

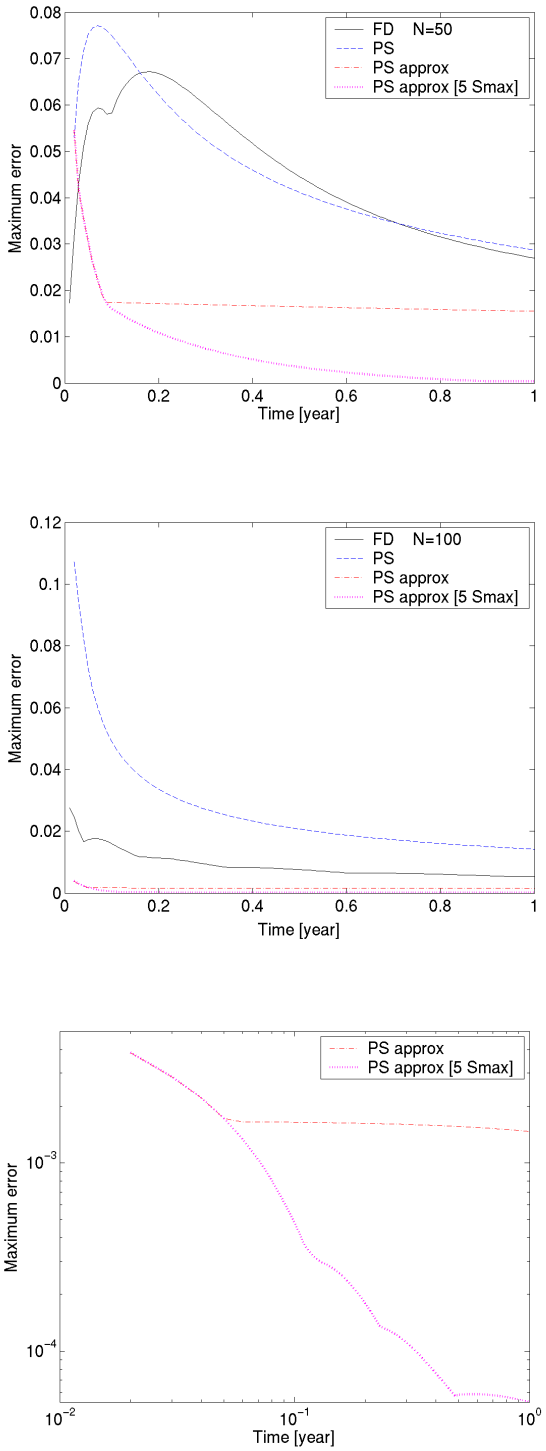

Figure 14: Maximum error as a function of time. The bottom figure is a magnification of the middle one but with logarithmic axis.

The errors in the solution are presented in Figure 15 below. As expected the maximum error for both FD and PS are situated in the region around K. But the maximum error in the solution for PS approximated IC has moved from K, where the maximum representation error where situated (Figure 17), to the beginning of the domain (for details see Figure 16).

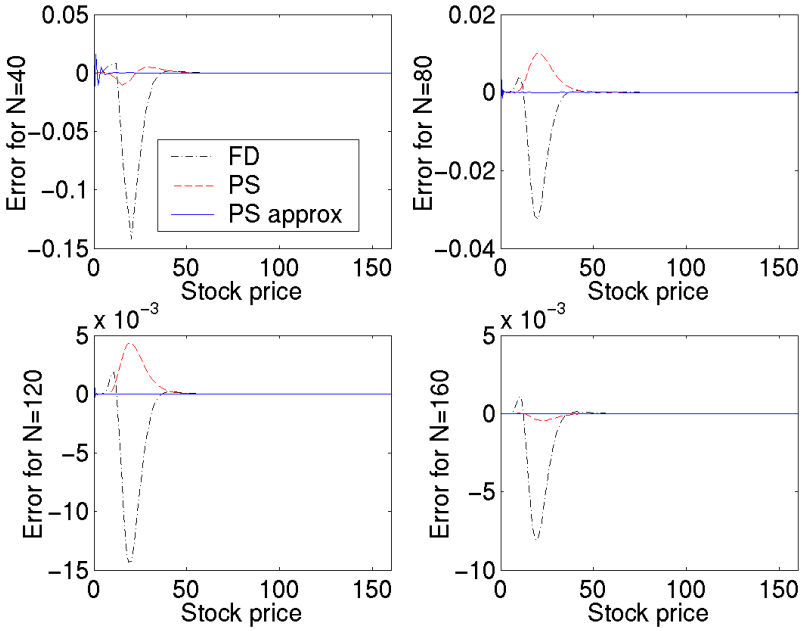

Figure 15: Error in solution for FD, PS and PS approximated IC. A magnification of the error for PS approximated IC is presented in Figure 16.

Figure 16 below shows the beginning of the domain for the case with PS approximated IC more detailed.

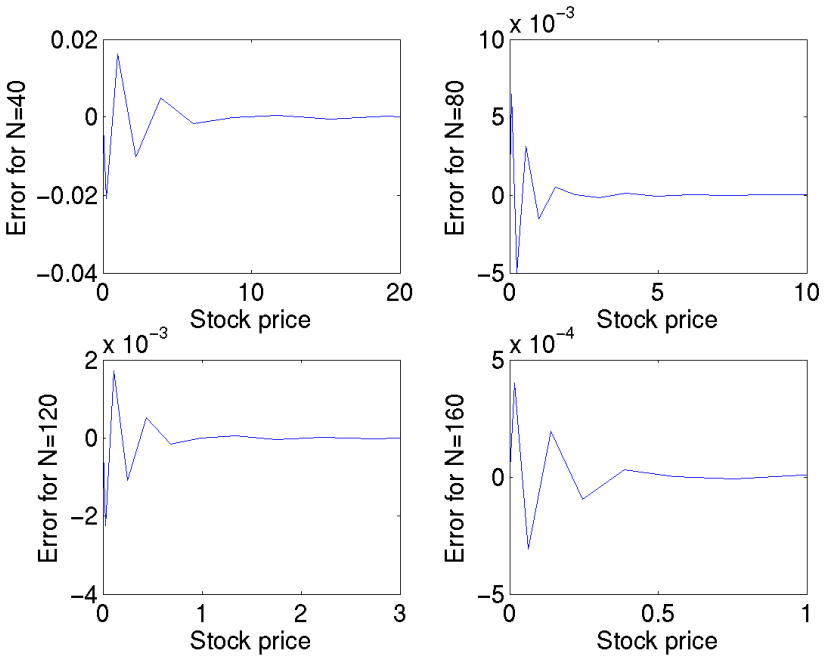

Figure 16: A magnification of Figure 15 showing the error in solution for PS approximated IC.

Figure 17 describes the transportation of the maximum error for PS approximated IC. 100 grid points and a time step of 0.005 were used.

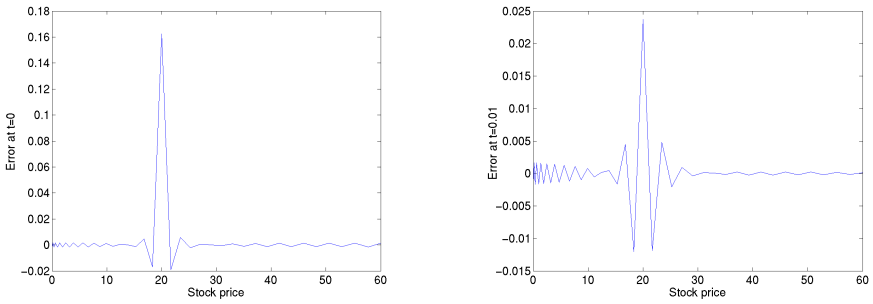

(a) 0 time iterations

(b) 2 time iterations

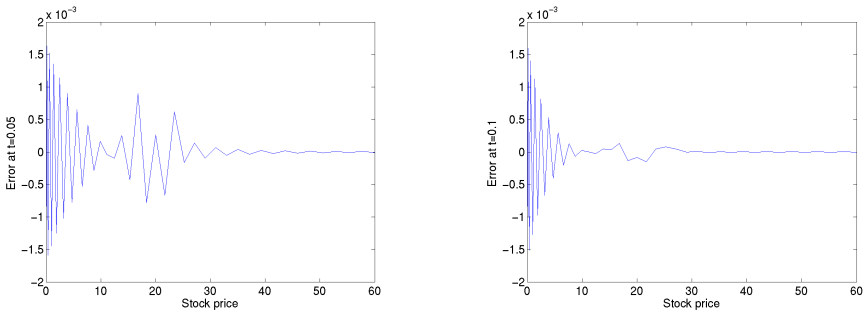

(c) 10 time iterations

(d) 20 time iterations

Figure 17: The development of the error for PS approximated IC.

To study the accuracy of the different methods, the maximum error as a function of the number of grid points are presented in Figure 18 for FD, PS and PS approximated IC.

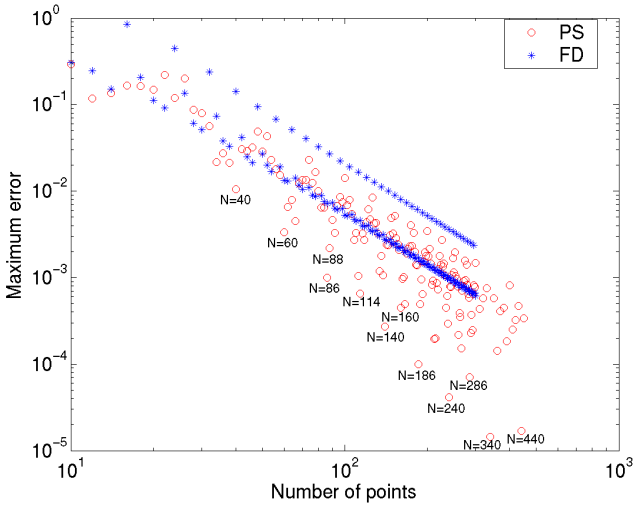

(a) Convergency rate for PS and FD.

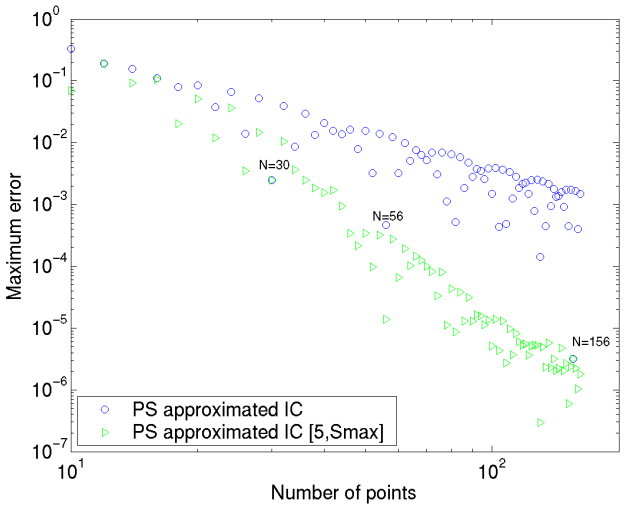

(b) Convergency rate for PS approximated IC

Figure 18: Convergence for FD, PS and PS approximated IC.

Figure 18(a) shows that the convergence rate for FD is of order 2, as expected from theory (see section 2.2) and is also shown in Figure 4. The convergence rate for PS is higher but it shows a very unpredictable oscillative behavior. The most successful points, the ones with the lowest maximum error, are of

certain interest. The convergence rate is approximately of order 3 for these points. In Figure 18(a) these points seem to have a repetitive cycle for every 100 point. This is not the focus of this work, and there probably exist strong correlation but this is not further examined here.

Figure 18(b) is the same as 18(a) but for PS approximated IC. The figure also shows the maximum error in the solution for PS approximated IC when the beginning of the domain is neglected. The largest errors for this method is, as showed in Figure 16, located in the beginning of the domain. The time step in Figure 18(b) is shortened from 0.01 to 0.001 because the error from the discretization in time starts affecting the maximum error significantly when the space discretization error is of order 10^{-5}. The convergence rate for PS approximated IC is at least of order 2 but when the domain is reduced to 5 to S_{max} the convergence rate is approximately 4.5.

Figure 18(b) shows that the error for PS approximated IC in the entire domain is particular small for $N = 30$, 56 and 156. Therefore the error as a function of the stock price is plotted for these N (left column of Figure 19) and for comparison the error is also plotted for $N + 1$ (right column of Figure 19), where the error is not particular small.

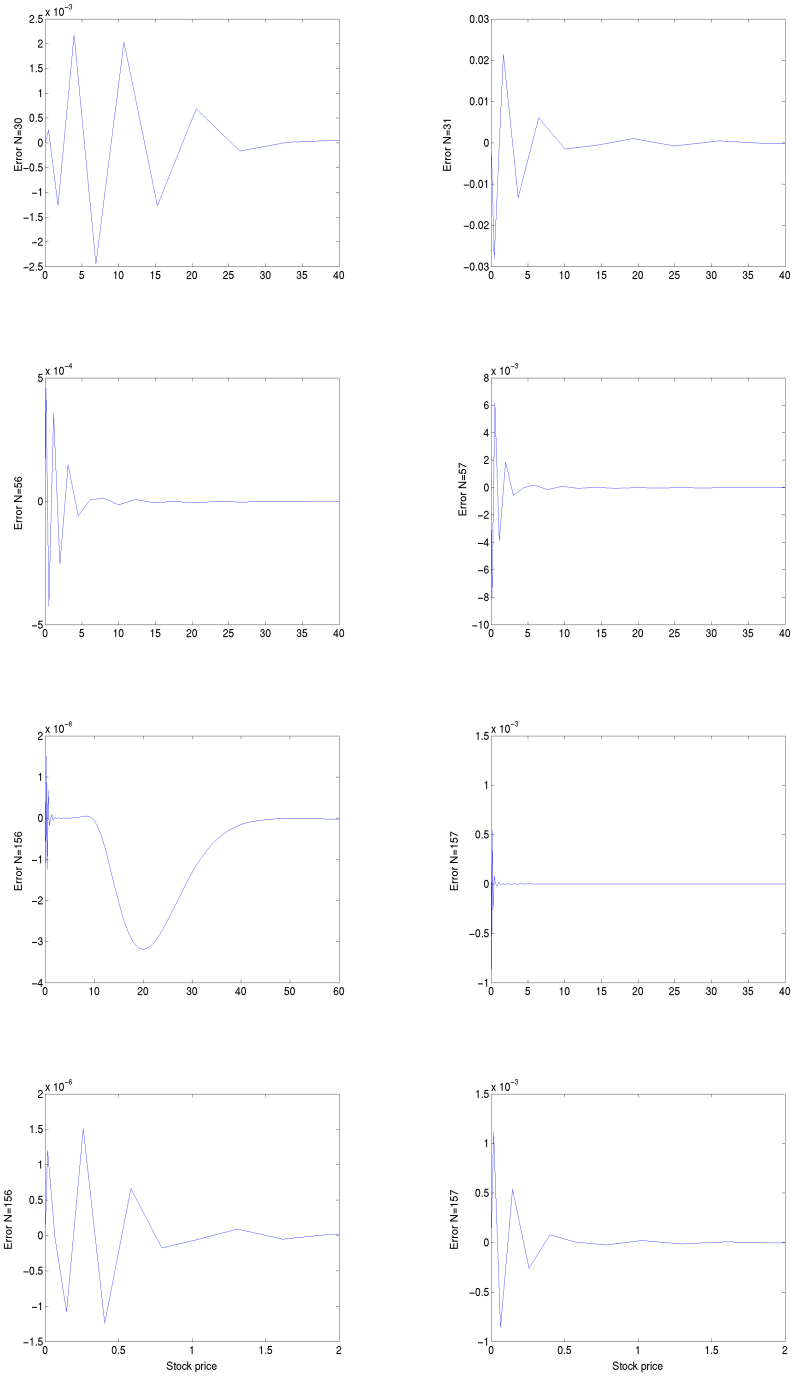

Figure 19: Error for PS approximated IC as a function of the stock price. The left column is for successful N and the right column is for N one bigger than the successful ones. Notice that there are two subfigures for the case when N equals 156 and 157, the two bottom ones are the magnification of the beginning of the domain.

The error in Figure 19 is located in the beginning of the domain. The error at the end of the domain is infinitesimal relative to the beginning and hence this region is excluded from the figures. It is interesting that a larger number of grid points does not necessarily result in a more accurate solution. The above mentioned points has the same magnitude of the error as the one with the decreased domain. It would be of interest to know why these points are so successful. A correlation to the representation error has not been found. The maximum error is the error studied and the successful points seem to have a large area of the error.

4 Results in two dimensions

Unfortunately an accurate solution of the two-dimensional Black–Scholes equation discretized with PS has not yet been implemented. The parameter values used were $\sigma_{11} = \sigma_{22} = 0.3$, $\sigma_{12} = \sigma_{21} = 0.05$, $\Delta\tau = 0.1$, $K = 20$, $S_{max1} = S_{max2} = 8K$, $T = 1$ year and $r = 0.05$.

The boundary condition used on boundary 1 and 2 were the analytic solution from equation (9). The boundaries and the points are defined according to Figure 20. In point B,

$$F(0, S_{max1}, S_{max2}) = \Big(\frac{S_{max1} + S_{max2}}{2} - Ke^{-r\tau}\Big),$$

was used. Boundary 3 is generated from the straight line between the function values of A and B. Analogously boundary 4 is determined with the help of the values of point B and C.

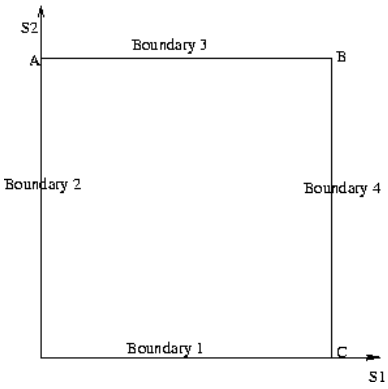

Figure 20: Definition of the boundaries.

In two dimensions it does not exist an analytic solution. Instead a numerical solution from FD was used as reference solution. The reference solution was

calculated with the time step $\Delta\tau = 0.01$. In space it used five times as many grid points as the solution for PS which it is compared with. The result below is for $N_1 = N_2 = 20$. Figure 21 shows that the solution with PS differs a lot from the solution with FD in the interesting region around K. The behavior is the same when a higher number of grid points and a smaller time step is used.

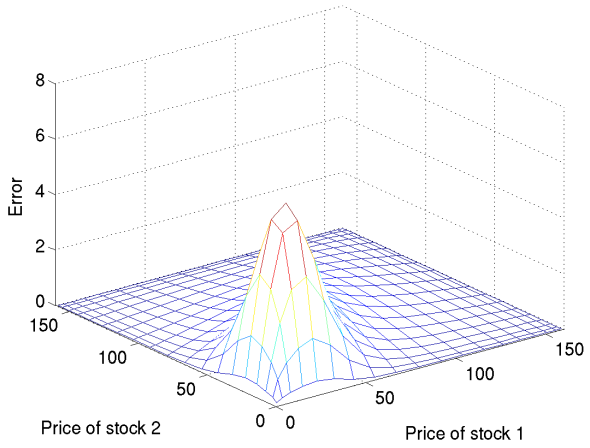

(a) 3-dimensional figure of the "error".

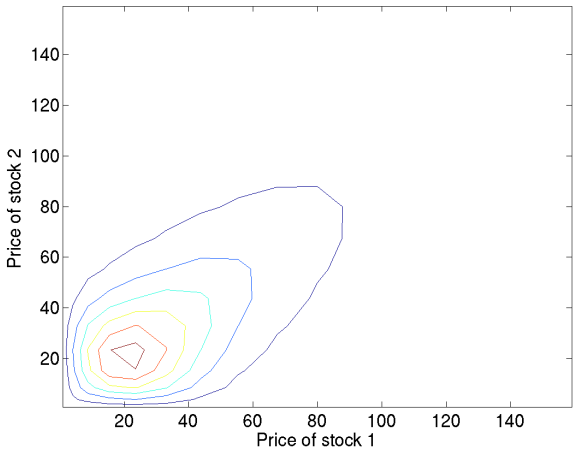

(b) Contour plot of the "error".

Figure 21: The difference between the solution for PS and FD.

5 Discussion

When solving Black–Scholes PDE with the use of FD or PS a system of equations needs to be solved for every iteration in time, because the time discretizing method is implicit. The difference between the two techniques is that the system of equations is tridiagonal, when FD is used for the spatial discretizing, hence $\mathcal{O}(N)$ operations is required to solve the system of equations. In comparison PS creates a dense system of equations that requires $\mathcal{O}(N^3)$ operations. Therefore the method of discretizing with PS is only useful in the case when a significantly less number of grid points in space is used to reach the same magnitude of the error. The results show that this criteria is not fulfilled except for a few set of grid points. These set of grid points is not examined in this work so further research would be of interest. If these set of points were known and easily applicable it would be of interest to further compare the accuracy and effectivity of PS compared to FD, for the mentioned points.

To achieve a better result with the same amount of arithmetic operations, the initial condition is approximated with a finer grid than the Chebyshev points. This is only done once and therefore adds an insignificant amount of work. But the result is impressive when the studied region excludes the beginning of the domain. The exclusion of the region in the beginning of the domain is not a big drawback, since the region close to the exercise price is of superior interest in financial mathematics. To achieve an error of the magnitude 10^{-3} FD require 240 grid points and PS, with the reduced domain, require 40 grid points. Further on, FD with 100 points result in an error of magnitude 10^{-2}, for the same number of grid points PS with the reduced domain gives an error of magnitude 10^{-5}. These results show that it is useful to solve Black–Scholes equation with PS with approximated IC, even though it requires more arithmetic operations than solved with FD. The high accuracy order when solved with PS with approximated IC is due to the behavior of the maximum error. When the solution is iterated forward in time the maximum error is transported from the region close to the exercise price to the region in the beginning of the domain.

Acknowledgments

Thanks to J. Persson and C. Peterson for their excellent guidance during the problem solving phase of the project and their constructive comments on the creation of this report.

References

[1] P. Wilmott, J. Dewynne, S. Howison, *Option Pricing: Matchematical Models and Computation*, Oxford Financial Press, Oxford, UK, 1993.

[2] Lloyd N. Trefethen, *Spectral Methods in Matlab*, SIAM (Society for Industrial and Applied Mathematics), Philadelphia, US, 2000.

[3] American Mathematical Society *The 1997 Nobel Prize in Economics*, http://www.ams.org/new-in-math/nobel1997econ.html

[4] Kevin Rubash *A Study of Option Pricing Models*, Bradley University. http://bradley.bradley.edu/ arr/bsm/model.html

[5] Bengt Fornberg, *A Practical Guide to Pseudospectral Methods*, Cambridge University Press, Cambridge, UK, 1998.

[6] T. Björk. *Arbitrage Theory in Continuous Time*, Oxford University Press, New York, 1998.

[7] J. Persson, L. von Sydow, *Pricing European Multi-asset Options Using a Space-time Adaptive FD-method*, Uppsala University, Technical report 2003-059, 2003.

[8] L. Råde, B. Westergren, *Mathematics Handbook for Science and Engineering BETA*, Studentlitteratur, Lund, 1998.

[9] *Mathworld a Wolfram web resource*, http://mathworld.wolfram.com/

[10] E. Kreyszig. *Introductory Functional Analysis with Applications*, Wiley, New York, 1989.